Relating physical and chemical properties of four different biochars and their application rate to biomass production of *Lolium perenne* on a Calcic Cambisol during a pot experiment of 79 days

José M. de la Rosa[1*], Marina Paneque[1], Ana Z. Miller[1,2], Heike Knicker[1]

1. Instituto de Recursos Naturales y Agrobiología de Sevilla (IRNAS-CSIC), Av. Reina Mercedes, 10, 41012, Seville (Spain).

2. CEPGIST/CERENA, Instituto Superior Técnico, Universidade de Lisboa. Av. Rovisco Pais, 1049-001, Lisbon (Portugal).

*corresponding author: jmrosa@irnase.csic.es; Tel. +34 954624711

Abstract

Three pyrolysis biochars (B1: wood, B2: paper-sludge, B3: sewage-sludge) and one kiln-biochar (B4: grapevine wood) were characterized by determining different chemical and physical properties which were related to the germination rates and to the plant biomass production during a pot experiment of 79 days in which a Calcic Cambisol from SW Spain was amended with 10, 20 and 40 t ha^{-1} of the four biochars.

Biochar 1, B2 and B4 revealed comparable elemental composition, pH, water holding capacity and ash content. The H/C and O/C atomic ratios suggested high aromaticity of all biochars, which was confirmed by ^{13}C solid-state NMR spectroscopy. The FT-IR spectra confirmed the aromaticity of all the biochars as well as several specific differences in their composition. The FESEM-EDS distinguished compositional and structural differences of the studied biochars such as macropores on the surface of B1, collapsed structures in B2, high

amount of mineral deposits (rich in Al, Si, Ca and Fe) and organic phases in B3 and vessel structures for B4.

Biochar amendment improved germination rates and soil fertility (excepting for B4), and had no negative pH impact on the already alkaline soil. Application of B3, the richest in minerals and nitrogen, resulted in the highest soil fertility. In this case, increase of the dose went along with an enhancement of plant production. Considering costs due to production and transport of biochar, for all used chars with the exception of B3, the application of 10 t ha^{-1} turned out as the most efficient for the crop and soil used in the present incubation experiment.

Highlights:

- Turning organic waste into biochar helps to improve soil fertility of Calcic Cambisols
- Kiln wood biochar resulted in low water retention capacity & specific surface area
- Feedstock drives the differences in the composition and functionalities of biochars
- 10 t biochar ha^{-1} was the most efficient dose for improving soil fertility

Keywords

Pyrolysis, kiln, biochar properties, pot experiments, soil amendment, specific surface area, *Lolium perenne* grass.

1 Introduction

Biochar is the product of thermal degradation of biomass in the absence of oxygen (pyrolysis) with the goal to be used as a soil amendment (Lehmann and Joseph, 2009).

Considering the increasing amount of organic agricultural and urban wastes, there is an urgent need for finding a sustainable strategy which allows managing and reducing these kinds of residues. The shift toward a biobased economy will probably promote the application of by-products from bioenergy productions as either soil amendments or fertilizers. In this sense, biochar has been proposed as a novel tool to achieve this goal. Biochars contain large amounts of C. Thus, when applied to land, they have the potential to significantly increase soil organic matter (SOM) contents. The latter is in critical decline in many regions of the world, particularly in agricultural areas of Mediterranean countries due to factors such as water shortage, overgrazing, intense agriculture and fire frequency. Specifically, biochar may offer a new strategy for restoring carbon to such depleted soils, and since biochar is considered to be more stable than SOM concomitantly sequestering significant amounts of CO_2. This is in accordance with the commitment of the European Community to lower its GHG emissions to 20% below their 1990 level by the year 2020.

Concerning agriculture, research has pointed to biochar as a new ecological amendment which may enhance soil quality and plant growth (Sohi et al., 2009). Biochar can act as a soil conditioner enhancing plant growth by supplying and, more importantly, retaining nutrients and by providing other

services such as improving soil physical and biological properties (Glaser et al., 2002; Lehmann et al., 2003). Evidences gathered from greenhouse and field trials indicate that biochar additions to soil can produce agricultural benefits (Ogawa and Okimori, 2010). However, the effectiveness of biochar in enhancing plant fertility is not only a function of soil type, climate, and type of crop (Blackwell et al., 2009) but also of the biochar properties. The inherent variability of biochars due to different feedstock and production conditions implies a high variability of their effect on soil properties and productivity. Not all biochars have demonstrated improved agricultural productivity in all cases (Van Zwieten et al., 2010). This strongly suggests that the production and use of biochars as soil improvers will need to be customized for each situation. Furthermore, due to the irreversibility of biochar application, it is necessary to perform detailed studies to achieve a high level of certainty that adding biochar to agricultural soils, for whatever reason, will not negatively affect soil health and productivity.

Therefore, the interest of our research was to improve our understanding how the properties of four biochars produced from different feedstock (conifer chip-wood, pulp paper sludge, sewage sludge and grapevine wood) are related to their potential to increase fertility of a typical Mediterranean soil. As a representative of such soils, we used material from Calcic Cambisol from the Guadalquivir river valley in Andalusia, Southern Spain and performed a pot experiment in which the impact of the addition of different doses of biochars on seed germination and plant growth was tested. Biochar has a number of properties that make its characterization analytically unique and challenging. In order to reveal the impact of the properties of the biochars on plant growth, they

were subjected to elemental analysis, microscopy and the determination of several chemical and physical properties such as, pH, ash content, water holding capacity (WHC) and surface area measurement (S_{BET}). Fourier-transform infrared spectroscopy (FT-IR) and ^{13}C solid-state nuclear magnetic resonance (NMR) techniques were also applied to elucidate the molecular structure and main chemical groups, whereas field emission scanning electron microscopy (FE-SEM) was valuable for investigating the surface topography, porous structure and chemical composition of biochars. Special attention has been devoted to the surface properties of biochars. The specific surface area drives the adsorptive ability of biochars for different soil components and consequently their capability to enhance soil fertility. This information may be used to guide the design and production of biochars to fulfill explicit purposes such as soil amelioration, soil remediation, or carbon sequestration (Mukherjee et al., 2014). However, there is presently very little published data detailing how the surface properties of biochar vary with biochar type, including production condition and parent biomass type (Weng et al., 2006)

2 Materials and Methods

2.1 Sample material

Three of the studied biochars were provided by the European Ring Trial, organized by the Biochar COST action TD1107 entitled "Biochar as option for sustainable resource management", and are derived from wood (B1), paper-sludge (B2), and sewage sludge (B3). The fourth sample, B4, was supplied by "Bodegas Torres" Company which produces biochar from the waste of the grapevine wood biomass which is older than 1 year by using the traditional

kilns. The production conditions, feedstock and the pyrolysis conditions of the four biochars are shown in Table 1. Biochars 1 to 3 were produced by Swiss Biochar, Sonnenerde GmbH and Pyreg companies respectively by a controlled pyrolysis process under similar conditions (temperature increasing from 20ºC to 500-620ºC; 20 minutes pyrolysis time; water content of 30%). In contrast, B4 was produced by using the centennial kiln methodology. After the pyrolysis process, all samples were homogenized and oven-dried at 40ºC during 72 hours. In the case of B4, due to the big size and heterogeneity of the fragments, the char was crushed and sieved (< 1 cm) to increase homogeneity of the material. Subsequently, all samples were kept in sealed untransparent plastic bags and maintained at 4ºC until they were used to avoid their alteration or microbial degradation.

2.2 Incubation experiment

The soil matrix used for the greenhouse incubation experiment was obtained from the A_h horizon of a typical Mediterranean agriculturally managed soil classified as Calcic Cambisol (IUSS Working Group WRB, 2007), it is a calcareous sandy loam soil located at the experimental station "*La Hampa*" of the *Instituto de Recursos Naturales y Agrobiología de Sevilla*, in the Guadalquivir river valley (SW Spain; 37º 21.32' N, 6º 4.07' W), Coria del Río, Seville. After sampling, the soil was dried at 40ºC, du ring 48 h, and sieved (<2 mm). Small branches, fresh mosses and plant remains, as well as roots were removed manually. The soil contains 20 g C kg^{-1} of which 7 g kg^{-1} is attributed to organic carbon and 1 g N kg^{-1}. Its pH in water is 8.6 and its WHC (according to Veihmeyer and Hendrickson, 1949) and ash content of 46% and 95.2%

respectively. Those parameters are typical values reported for Cambisols of cultivated areas around Aljarafe which is located within the province of Seville (Mudarra-Gómez, 1988).

The pots for the incubation experiment were prepared as follows: the 250 mL plastic containers (16 cm height) were perforated to allow leaching of surplus water during the experiment; 120 g of soil were placed in each pot and 40 certified grass seeds (*Lolium perenne*-ILURO seeds company, Spain) were added. Separately, 30 g of soil were mixed with amounts equivalent to 10, 20 and 40 t ha^{-1} of each biochar and the mixture was laid above the pure soil matrix. Thus, biochar amendment was solely applied to the top 5 cm of each pot, approximating the way farmers usually manage such organic amendments. For each application rate and biochar four replicates were prepared (n= 4). Additionally, 6 pots without any biochar amendment were used as control (n= 6). After adjusting the soil humidity to 60% of the maximum WHC, the pots were placed into a greenhouse at 25ºC and 14 h light day^{-1} for 79 days. No mineral nutrient solution was added. The samples were irrigated regularly during the whole experiment. The amount of applied water accounted to 166 L m^{-2}, which is equivalent to 760 L m^{-2} per year, similar to the annual average precipitation in this region. The number of living grass shoots was counted after 6, 8, 10, 16, 23, 30, 37, 51, 65 and 78 days of the incubation in order to assess the effect of the kind and amount of each biochar on the germination of the seeds and on the plant-survival. In addition, for assessing the biomass production, the shoots were cut, dried (48 h at 40ºC) and weighed after 21, 35, 51, 65 and 79 days of incubation.

The response variables for the germination of the seeds and plant-survival were transformed prior statistical analysis to normalize data distribution. Square roots of percentages of germination and survival data were carried out according to Fernández et al. (2010). Total grass biomass (dry weight in mg) per pot was used as response variable for biomass production. Percent germination and percent survival data met ANOVA assumptions, thus they were analyzed by ANOVA. Tukey test was used in the cases it was necessary. Total grass biomass per pot data violated ANOVA assumptions, thus in this case the Kruskal-Wallis non-parametric test followed by the Mann-Whitney's U non-parametric test were applied. All the statistical analyses of the number of germinated seeds and plant biomass were carried out by using SPSS version 17.0 (SPSS, Chicago, IL, USA). Kolmogorov-Smirnov non-parametric test was used to test for normality and Levene to test for homogeneity of variance for all parameters. All the *p* values were considered to be significant at $p \leq 0.05$.

2.3 Determination of chemical and physical parameters

2.3.1 Elemental analysis

Total carbon (TC), hydrogen (H) and nitrogen (N) concentrations were determined in triplicate of the bulk soil and the biochars by dry combustion (1000ºC) using a Perkin-Elmer 2400 series 2 elemental analyzer. Samples were grounded to 1 mm and dried (105ºC, 6 h) before analysis. The total organic carbon (TOC) content of the soil was calculated from the residual C which remained after removal of carbonates with 2 M HCl. The coefficient of variation of replicated analyses was below 5%.

2.3.2 Ash content

For the measurement of the ash content, the method of ASTM D 2974-87, originally designed for its application to peats and other organic soils, was adapted to biochar samples. Briefly, after drying at 105℃ for 5 hours, 0.30 g of each biochar were placed in a porcelain crucible and heated in a muffle furnace at 750℃ during 5 hours. The remaining ash was weight ed and its amount was related to the mass of the oven-dried sample. Each sample was analyzed in triplicate.

2.3.3 pH value

For the soil sample, the standard soil:water ratio of 1:2.5 was used. The mixture was shaken and after settling for 60 min. The pH of the suspension was measured with a pH meter (Multimeter MM40, CRISON) in triplicate. In order to obtain a homogenous suspension for the biochars the biochar:water ratio had to be increased to 1:10. Otherwise, those samples were treated in a similar way than previously explained.

2.3.4. Water Holding Capacity (WHC)

The WHC was determined by placing 6 g of each biochar over a filter paper (Whatman 2) into a funnel. After saturation of the biochar with distilled water and letting the covered funnels stand for 12 hours the moist weight of the sample was calculated considering the weight of the funnel and the filter paper. The weight difference between the sample before and after water addition and settling for 12 hours yielded the maximal WHC. It is expressed as the

percentage relatively to the total dry weight of the sample. The WHC was determined for each biochar sample and the bulk Cambisol in triplicate.

2.3.5 Specific surface areas (SSA_{BET})

Specific surface areas (SSA_{BET}) were measured by adsorption of an ultra-high purity gaseous N_2 at liquid nitrogen temperature (77 K) using an NOVA 2200e surface area analyzer (Quantachrome Instrument Corp., Boynton Beach, FL). Prior to the surface area measurements all the samples were outgassed in sample tubes at 60°C under continuous N_2 gas flow for ~12h. The adequacy of degassing times was validated using the method described in the ASTM D4820-97 for black carbon N_2 adsorption measurements. SSA_{BET} were calculated based on Brunauer et al. (1938). All N_2 measurements were performed in triplicate (n= 3).

2.4 Spectroscopic analysis

2.4.1 ^{13}C Solid-State NMR Spectroscopy

Prior to NMR analysis, the biochar samples were treated with HCl (2M) to reduce the content of paramagnetic compounds. Before NMR analysis samples were washed with distilled water and dried. The ^{13}C solid-state NMR spectra were obtained with a Bruker Avance III 600 MHz wideboard spectrometer operating at a ^{13}C resonance frequency of 150.93 MHz. Grained and homogenized sample material was placed into zirconium rotors of 4 mm OD with KEL-F-caps. The cross polarization magic angle spinning (CPMAS) technique was applied with a spinning speed of 14 kHz. A ramped ^{1}H-pulse was used during a contact time of 1 ms in order to circumvent loss of selective signal

intensity due to spin modulation during the Hartmann-Hahn contact. The ^{13}C-chemical shifts were calibrated relative to tetramethylsilane (= 0 ppm) with glycine (176.04 ppm). Approximately 10,000 single scans with pulse delays between 300 and 500 ms were accumulated for each spectrum.

A ^{13}C NMR spectrum of B1 could not be acquired because the electrical shielding (skin effect) of its graphenic network caused strong reflection of the irradiation pulse and prevented correct tuning of the probe. This reflection can lead to a heating up of the electronics and thus can cause major damage of the equipment.

Table 2 shows the tentative assignment of the typical chemical shift regions of the ^{13}C solid-state NMR spectra of soil samples to C groups. The ^{13}C intensity distribution was obtained by an integration routine with MestReNova 7 Software ®. The spinning speed of 14 kHz was not sufficient for complete removal of the chemical shift anisotropy of the aromatic carbons, which caused spinning side bands to occur at both sides of the parent material at a distance of the spinning speed (here between 210 and 185 ppm and between 45 and 0 ppm). Their intensities (2 times the region between 210 and 185 ppm) were added to that of the parent signal between 160 and 90 ppm. Respectively, the intensity of the alkyl region was corrected according to Knicker et al (2005).

2.4.2 Fourier Transform Infrared Spectroscopy (FT-IR)

The FT-IR spectra were recorded using a JASCO 4100 spectrometer at wave lengths ranging from 4000 to 400 cm^{-1} and a resolution of 2 cm^{-1}. Potassium bromide pellets containing about 1% (w/w) of each biochar were prepared in a cylindrical piston under high pressure and vacuum. In order to improve the

signal to noise ratio, 60 scans were registered and accumulated for each recorded spectrum. Spectra of samples were corrected against a pure KBr pellet prior to every measurement. All IR data manipulations were performed using JASCO spectra manager software ®.

2.5 Field emission scanning electron microscopy (FESEM)

Bulk biochar fragments were directly mounted on a sample stub and sputter coated with a thin gold/palladium film. Subsequently, samples were examined on a Jeol JSM-7001F microscope equipped with an Oxford X-ray energy dispersive spectroscopy (EDS) detector using standard ZAF corrections that allow semi-quantitative microanalysis. FESEM examinations were operated in secondary electron (SE) detection mode with an acceleration potential of 15 kV.

3 Results and discussion

3.1 Elemental composition of biochars

Biochar 1 and B4, both produced from wood, show comparable C contents of approximately 750 g kg^{-1}. Lower C contents (509 g kg^{-1}) were determined for B2, which derived from paper-sludge, and B3 (179 g kg^{-1}), produced from sewage sludge. Comparable values were reported previously (Zhao et al., 2013; Agrafioti et al., 2013). Considering that B1 to B3 were produced under similar pyrolysis conditions (Table 1), our data confirm that the C content of biochar depends strongly on the feedstock (Zhao et al., 2013). Biochars produced from wood biomass usually contain carbon amounts higher than 500 g kg^{-1}, because the original biomass is rich in carbon compounds which are not easily degraded during heat like lignin (Sharma et al., 2004; Ho Kim et al.,

2012) or form heat-resistant charring products such as furans derived from cellulose.

The N contents of the wood biochars, B1 and B4, are within the range reported previously (Enders et al., 2012), but are lower than those of B2 and B3 (Table 3). The high N content of B3 is similar to the values found for other sewage sludge charcoals (Zaho et al., 2013) and is best explained by the fact that the organic material of the feedstock is rich in peptide-like compounds which are transformed into N-heteraromatic structures during thermal treatment (Knicker, 2010). These findings reveal that the organic matter content and thus the N concentration of the four biochars studied are influenced mainly by the C/N ratios of the source material, regardless of the pyrolysis conditions. Biochar 1 yields an atomic H/C ratio of 0.3, which is close to that of B2 and B4 and is related to a high condensation degree. In contrast, a value of 0.9 indicative for a high protonation was obtained for B3 (Knicker et al., 2005; Hammes et al., 2006). However, one has to bear in mind that this sample contains silicates which may have contributed to increase both its O and H contents.

With respect to the atomic O/C ratio, B1 shows the lowest value, followed closely by B4. The higher values of 0.3 and 0.4 observed for B2 and B3 respectively indicate the presence of polar functional groups and O-containing heterocyclic compounds, which may increase their hydrophilic properties (Schimmelpfenning and Glaser, 2012).

Plotting the atomic H/C and O/C ratios into a van Krevelen diagram to elucidate the carbonization degree of the samples, confirms that B1 and B4 and are formed by highly condensed hydrocarbons which is commonly yielded in wood biochar samples produced at elevated temperatures (Supplementary Fig. 1).

Correspondently, B3 shows values typical of low condensed organic matter with similar H/C and O/C ratios to lignin material. However, as mentioned above, here the contribution of mineral matter may obscure the values.

3.2 Physical properties of biochars

Biochar 3 contains considerably higher amount of ash than the other samples (~70%). In general the ash contents of the biochars used in this study were in the range expected for the respective feedstock (Enders et al., 2012; Zaho et al., 2013).

The pH values of B1, B2 and B4 are around 10, and 6.7 for B3. Agrafioti et al. (2013) reported a pH around 6 for biochars derived from sewage-sludge. In contrast to the data obtained here, some works reported a positive relationship between ash content and pH values. This is probably due to the special composition of ashes from sewage sludge. In general, the main components of the ash are usually salts of alkali and alkaline elements (Na, K, Ca, Mg) but sewage-sludge can have a high concentration of heavy metals or silicates which remain mostly as part of the ash after the pyrolysation process (Agrafioti et al., 2013) but are not increasing the pH. Despite the different pH values of biochars and the used Cambisol, biochar addition did not alter significantly the pH of soils after 79 days of incubation. The pots amended with B3 resulted in pH 8.4-8.5, it ranged 8.6 to 8.7 for the rest of the biochar amended soils, whereas the pH of biochar un-amended pots was 8.5. Those values suggest that under these conditions, (79 days of incubation with a regular water supply and constant temperature) the pH of the studied calcic Cambisol was not disturbed by biochar addition.

A positive correlation between carbon content and WHC was observed for all biochars (r= 0.823; p 0.05). Thus, B1 exhibits the highest WHC (and C content), followed by B2. According to its OC content B4 showed a lower WHC than expected.

In our study, even though biochars 1-3 were produced under comparable pyrolytic conditions, their SSA_{BET} are varying from > 400 $m^2 g^{-1}$ for B1, to 67.3 $m^2 g^{-1}$ for B3, which indicates the strong impact of the nature of the feedstock on this parameter. The extremely low SSA of B4 ($SSA_{BET} \leq 5$ $m^2 g^{-1}$; Table 3) is probably related to the production conditions (traditional kiln method). Nevertheless, it has to be stated that the standard analytical methods assigned to surface area are techniques developed and optimized for materials other than biochars. The N_2 BET method was developed to characterize catalyst supports and other rigid matrix materials, such as zeolites. For instance, in the case of samples with a majority of highly microporous carbons, CO_2 at 0ºC is a better adsorbent and provides more reliable measurements than N_2 at -196ºC because of the higher testing temperature.

3.3 ^{13}C Solid-State NMR Spectroscopy

Figure 1 shows the ^{13}C NMR spectra of B2, B3 and B4 and their intensity distribution after considering the spinning side bands. Most likely due to the high condensation degree of the aromatic network in B1, tuning of the NMR probe was not possible for this material and no ^{13}C NMR spectrum could be acquired. Aryl C (160-90 ppm) represents the dominating C form in all biochars (Fig. 1). Biochar 2 and B4 exhibit with more than 80% of the total ^{13}C intensity assignable to this compound class, the highest aromaticity, whereas in B3,

approximately 71% of the total C occurs as aryl C. The dominance of aryl C in charcoals is also reported by other authors (De la Rosa and Knicker, 2011; Wu et al., 2012). However, here one has to bear in mind that the aryl C region covers the resonance lines not only of benzylic ring C but a broad range of different aromatic structures including heteroaromatic compounds which cannot be assigned in more detail due to the broadness of the signal. On the other hand, combining the pattern of the NMR spectra with elemental analysis reveals some additional information. For example the low H/C ratios of B1 and B4 indicate the presence of graphitic structures. On the contrary, the high N content of B3 suggests high contributions of N heterocyclic aromatic C derived from the heat transformation of peptideous material typically found in in sewage sludge. Recent studies on proteinaceous samples showed that some peptides are cyclized at moderate pyrolysis temperatures (Knicker, 2010). Their signals are likely to contribute to the alkyl C region (45-0 ppm) of the ^{13}C NMR spectrum of B3. The spectra of B2, B3 and B4 show shoulders at 143, 152 and 151 ppm, respectively, which are typical for O- and N-substituted aryl C. They may derive from partially degraded lignin, furfurals or N-heteroaromatic structures (Knicker et al., 2005). A further resonance line is detected at 81 ppm in the spectra of B3 which may derive from surviving ether bonds.

In the region assigned to carboxyl/amide C group (185-160 ppm) the spectrum of B3 shows a slightly higher intensity percentage than those obtained from B2 and B4 (5% vs. 1%).

3.4 Fourier Transform Infrared (FT-IR) Spectroscopy

Figure 2 presents the FT-IR spectra of the four biochars. They confirm that, in general, B1, B2 and B4 are composed of similar functional groups whereas for B3 a few differences are detected. The peaks appearing in the spectra of all biochars at around 3600 cm^{-1} and 3350 cm^{-1} are assigned to O-H vibrations (Hossain et al., 2011). The broad signals around 3000-3100 cm^{-1} can be attributed to aromatic C-H groups (Schnitzer, 1978). However, one has to bear in mind that signals corresponding to O-H can attribute to this band. The peak at 1690 cm^{-1} (1695 cm^{-1} for B3) is usually assigned in biochar samples to aromatic C=C bending and alkene C=C stretching.

The FT-IR spectrum of B3 exhibits a further shoulder centered at 3274 cm^{-1}. Such a line has also been observed in IR spectra of other sewage sludge biochars (Hossain et al., 2011) and can be assigned to N-H vibration or to O-H stretching caused by moisture. Considering that B3 is rich in nitrogen an assignment of this band to the first seems to be more plausible. In the FT-IR spectrum of B1 a further signal can be seen at 1551 cm^{-1}, which is typically indicative for graphite moieties (Francioso et al., 2011). Its presence solely in B1 confirms the high condensation degree of this sample already concluded from the low H/C atomic ratio and the inability to tune the NMR probe prior to recording its ^{13}C NMR spectrum.

The spectra of B2, B3 and B4 reveal a band centered at about 1580-1585 cm^{-1} which is attributable to aromatic C=C vibration, possibly formed by heat induced dehydration of cellulose, and to aromatic C=O vibrations (Wu et al., 2012). This signal was shown to decrease with rising temperature by Zhao et al. (2013), which could explain the high intensity of this band in the spectra of B4, which has been produced at mild temperatures. The band at 1430 cm^{-1} in the spectra

of all biochars is typically assigned to aromatic C=C skeletal vibrations. This signal is shifted to 1434 cm^{-1} in the spectra of B3. Zhao et al. (2013) observed that the wavelength of this signal exhibits great variations when comparing biochars from different feedstock but remained almost unaltered when changing the production temperature. On the other hand this peak can also be assigned to asymmetric stretching of COO^- (Schnitzer, 1978). In the IR spectrum of biochar 4 appears a further signal at 1220 cm^{-1}, which was not identified in the remaining spectra and may correspond to R-OH and phenol groups. Possibly they were formed during charring of lignin when methoxyl C is transferred into hydroxyl groups and biphenyls are produced (Knicker, 2011). The lack of such a band in the spectrum of the other plant derived biochar (B1) may be explained with the different pyrolysis conditions during biochar production. The latter may have resulted in a complete transformation of the aromatic core of lignin whereas the milder conditions applied for the production of B4 allowed the survival of some lignin derivatives. This supports the conclusion that pyrolysis conditions affected considerably the molecular composition and functionalities of biochars and consequently its properties. The spectra of B2 and B3 show a band at 1065-1070 cm^{-1} which can be caused by Si-O-Si vibrations or by C-O stretching vibrations in polysaccharides (cellulose and hemicellulose) or in pyranoses and furanoses derived from of heat-altered cellulose and hemicellulose. Peaks appearing below 1000 cm^{-1} correspond to the bands of the out of plane bending for CO_3^{2-}. Part of these signals could be due to bending of C-H aromatic out of the plane (900-650 cm^{-1}) (Zaho et al., 2013; Wu et al., 2012).

3.5 FESEM-EDS analysis

Detailed FESEM images showed that indeed the biochar samples derived from different feedstock. Moreover, the porous structure of the biochar samples was clearly appreciable by FESEM, revealing a variety of pore structures, which vary with feedstock type and pyrolysis conditions (Downie et al. 2009). Macro-pores (> 10 μm) were clearly observed in B1, corresponding to hollow fibers (Fig. 3A, B). This is consistent with the findings from specific surface area measurement. Around and inside pores, mineral crystals were observed. The EDS punctual analysis performed on the mineral grains identified calcium as the major element, which points out to be calcite, probably from the ash fraction. In fact, all biochar samples contain high levels of Ca (Fig. 4).

FESEM images of B2 revealed great amounts of collapsed structures on the biochar surface derived from cellulose and plant-derived fibers (Fig. 3C). A magnified FESEM image of one remain of vessel structures is shown in Figure 3D. A complex network of pores of different diameter is also noticed, which is consistent with the relatively high surface area of this biochar. In contrast, B3 showed heterogeneous composition, with several collapsed structures and mineral deposits randomly distributed on its surface (Fig. 3E,F). A higher magnification FESEM image of Fe-mineral particles on the surface of B3 is shown in Fig. 3F. The EDS spectrum performed on the surface of this sample revealed great mineral diversity, which include Al, Si, P, K, Ca and Fe (Fig.4C). The concentration of Al and Si indicates the presence of clay minerals, whereas the Fe content (Fig. 4) and the morphology of these Fe-rich particles suggest being Fe oxides (Fig. 3F). In addition, the high level of P based on the EDS spectrum (Fig. 4C), suggests the presence of phosphates, which derive from

sewage or other organic waste (Srinath and Pillai, 1966). This chemical composition is consistent with the original biomass (sewage sludge). In addition, the content of inorganic elements, associated with the ash fraction, is in fair agreement with the significant ash content obtained for this biochar.

FESEM images of B4 showed good anatomical preservation of the vineyard wood feedstock, with abundant macropores and very scarce micropores (Fig. 3G). Xylem vessels with scalariform perforation plates from stem plant are observed (Fig. 3H). This structure is typical for biochar from wood-derived feedstock, the chemical composition of which is confirmed by EDS microanalysis. The high intensity of the C peak is typical of wood biochar (Fig. 4D). This is in agreement with previous results for wood biochars produced above 500ºC, which according to Macias and Arbestain (2010), are predominated by condensed aromatic carbon.

3.6 Seed germination and plant survival

Figure 5 depicts the number of plants which germinated and survived during the whole incubation time. After 5 days of incubation the four 10 t ha^{-1} biochar-amended treatments resulted in a significantly higher amount of germinated plants than the un-amended pots. The plants of the pots amended with 20 t and 40 t ha^{-1} responded comparable to those of the control. Possibly, greater application dose alters the soil properties negatively which affects the germination rates. Alternatively, with the high application rate, the concentration of allelophatic compounds of the biochars reached levels which were toxic for the plants. In addition, the pH of the calcic Cambisol was already alkaline, thus the high pH of B1, B2 and B4 (>10) may have caused a negative effect on

germination after soil amendment with high doses of biochar. In line with the previous findings, the highest germination rates were reached with application rates of 10 and 20 t ha^{-1}. The negative effect of such high doses was especially evident in the pots amended with 40 t ha^{-1} of B2 and B4, in which fewer number of plant seeds germinated plants than in the control. De la Rosa et al. (2013) reported also a negative effect on germination with elevated doses of N-ammonoxidized lignin, which was explained by elevated salt concentration and possible occurrence of allelophatic compounds. Van Zwieten et al. (2010) observed that germination of wheat in a Ferralsol significantly improved in the presence of two paper-mill biochars at 10 t ha^{-1} although other treatments within the same study did not affect the germination rates. The number of plant shoots reached the maximum (over 75%) after 16 days of incubation and no retardation effect was observed within the biochar amended pots in all treatments. Significant differences between the four biochars or doses were not observed.

After that, the number of living plants decreased quickly until day 51. Then the plants dying slowed down. By the end of the experiment the number of living plants for all biochar amended treatments at all doses were significantly higher than in the un-amended pots. For B1, B2 and B4 the best survival rates were obtained at application rates of 10 and 20 t ha^{-1}. In the case of B3, 20 and 40 t ha^{-1} resulted in the highest proportions of living plants. Statistical analysis confirmed the tendency observed with respect to germination and number of active plant shoots. The latter were significantly greater for biochars 1, 2 and 3 amended pots than the control ones, whereas the response of biochar 4 did not show significant differences when compared to the control (Figure 5).

3.7 Plant biomass productivity

Figure 6 shows the plant biomass produced per pot during the 79 days of the incubation. For all experiments, biochar amendment increased significantly the productivity compared to the un-amended pots. Amendments of B1, B2 and B3 yielded the highest plant biomass production (100-130 mg), which constitutes four times higher production of plant material than of the control (approx. 30 mg). In contrast, B4 amendment only increased the production from 2 to 3 times when compared to the control pots (50-85 mg versus 30 mg). The latter is most tentatively due to its low WHC, little SSA_{BET} and its pore structure shown by SEM. These surface characteristics are expected to cause also a low capacity for retaining soil nutrients and for improving the soil structure.

Increases of the plant production achieved by addition of biochars in the present experiment are higher than those reported recently by Schimmelpfennig et al (2014), which ranged 32-42% for incubated biochar amended pots. However, comparable high values were stated previously (Kishimoto and Sugiura, 1985; +224%, 0.5 t ha^{-1}; Chan et al., 2007; +130%, 100 t ha^{-1}; Major et al., 2007; +378%, 26 t ha^{-1}). With respect to the soil of our study, one has also to bear in mind that it is a sandy clay loam soil with very low TOC content. Thus it is expected that any addition of organic material with a high surface area can considerably increase its WHC and prevents the leaching of a significant fraction of the available nutrients. In particular during the hot and dry summers of the Mediterranean regions, this improvement certainly plays an essential role for enhanced fertility of such soils. This may already be reached with the addition of non-charred organic residues as it was demonstrated by Madejon et

al (2001), who achieved plant production increases of up to +250% by applying different organic amendments. However, replacing such amendments by biochar may be beneficial if the additional C-sequestration potential of the latter is taken into account.

Concerning the doses, the four biochars produced statistically comparable amounts of biomass for application doses of 10 and 20 t ha^{-1}. However, at the highest dose (40 t ha^{-1}), the productivity of biochars 1, 2 and 4 decreased. This trend may be a consequence of a higher availability of allelopathic compounds and the high pH of those biochars, which may affect plant survival. In contrast, the higher the dose applied of B3 the higher the amount of biomass, although once again the difference was not significant. This slight increase may be due to the notable presence of plant nutrients (including P and K) within the mineral fraction of B3 (see FESEM-EDS results).

4 Conclusions

The results presented above suggest that amendment of a Calcic Cambisol with four different biochars increased significantly the plant biomass production in all the cases. However, traditionally kiln pyrolysis method affected negatively the surficial properties and water retention capacity of wood biochar, which contributed to its lower capacity to retain soil nutrients and to improve the structure of the soil than the other biochars. Our study confirmed that the nature of the feedstock is the key factor for understanding the differences in the elemental composition and functionalities of the biochars. Those differences have an impact on the performance of the various biochars as soil amendment

suitable for increasing plant production. Considering the different properties, the success of our biochars as soil ameliorants was related mostly to their surface characteristics. However, the high presence of minerals, P and N in B3 is most likely the reason for the fact that its amendment yielded in the highest biomass production rates. A further important outcome of our study is that in the case of B1, B2 and B4 the attitude "add more – get more" will not yield in the wanted result. In contrast and considering costs for production biochar, its transport and subsequent application to the field, the dose of 10 t ha^{-1} turns out to be the most efficient one from the three tested doses. However, authors are conscious that other soils and other crops may lead to other recommended doses.

Acknowledgements:

The Marie Curie Actions of the European Union's Seventh Framework People Programme (REA grant agreement nº PCIG12-GA-2012-333784-Biocharisma project), the Spanish Ministry of Economy and Competitiveness (MINECO GCL2012-37041)) and the European Regional Development Fund (FEDER) are thanked for the financial support of the present study. Ph.D. J.M. De la Rosa was the recipient of a fellowship from the CSIC JAE-Doc program co-financed by the European Social Fund (JAE-DOC-056). Ph.D. Markus Kleber (Oregon State University, USA) is acknowledged for the Specific Surface Area analyses, the European Biochar Network (Biochar as option for sustainable resource management-COST action TD1107) and Bodegas Torres (Spain) for providing the biochar samples and Hans-Peter Schmidt (Ithaka Institute, Switzerland) for helpful comments. The "CITIUS" research center of the University of Seville

(Spain) is thanked for providing access to their Nuclear Magnetic Resonance Spectroscopy facility.

References

Agrafioti E., Bouras G., Kalderis D., Diamadopoulos E., 2013. Biochar production by sewage sludge pyrolysis. J. Anal. Appl. Pyrol. 101, 72-78.

ASTM D 2974-87, Standard Test Methods for Moisture, Ash, and Organic Matter of Peat and Other Organic Soils, ASTM, USA, 1993.

Blackwell P, Riethmuller G., Collins M. 2009. Biochar Application in Soil, in Lehmann J, Joseph S. Earthscan (Eds.), Biochar for Environmental Management: Science and Technology, London.

Brunauer, S., Emmett, P.H., Teller, E., 1938. Adsorption of gases in multimolecular layers. J. Am. Chem. Soc. 60, 309-319.

Chan K.Y., Van Zwieten L., Meszaros I., Downie A., Joseph S., 2007. Agronomic values of green waste biochar as a soil amendment', Australian J. of Soil Res. 45, 629-634.

De la Rosa J.M., Knicker H., 2011. Bioavailability of N released from N-rich pyrogenic organic matter: An incubation study. Soil Biol. Biochem. 43, 2368-2373.

Downie A., Crosky A. Munroe P., 2009. Physical properties of biochar, in Lehmann J., Joseph S. (Eds), Biochar for environmental management: science and technology, Earthscan, 13-32.

Enders A., Hanley K., Whitman T., Joseph S., Lehmann J., 2012. Characterization of biochars to evaluate recalcitrance and agronomic performance. Bioresource. Technol. 114, 644-653.

Francioso O., Sanchez-Cortez S., Bonora S., Roldán M.E., Certini G., 2011. Structural characterization of charcoal size-fractions from a burnt Pinus pinea forest by FT-IR, Raman and surface-enhanced Raman spectroscopies. J. Mol. Struct. 994, 155-162.

Fernández R., Trapero A., Domínguez J., 2010. Análisis de la varianza. In "Experimentación en agricultura". Consejería de Agricultura y Pesca, Servicio de Publicaciones y Divulgación, Seville. Spain. ISBN: 978-84-8474-281-4.

Glaser B., Lehmann J., Zech W. ,2002. Ameliorating physical and chemical properties of highly weathered soils in the tropics with charcoal - A review. Biol. Fert. Soils. 35, 219-230.

Hammes K., Smernik R.J., Skjemstad J.O., Herzog A., Vogt U.F., Schmidt M.W.I., 2006. Synthesis and characterisation of laboratory-charred grass straw (Oryza sativa) and chestnut wood (Castanea sativa) as reference materials for black carbon quantification. Org. Geochem. 37, 1629-1633.

Ho Kim K., Kim J-Y., Cho,T-S., Choi J.W., 2012. Influence of pyrolysis temperature on physicochemical properties of biochar obtained from the fast pyrolysis of pitch pine (*Pinus rigida*). Biores- Technol. 118, 158-162.

Hossain M.K., Strezov V., Chan K.Y., Ziolkowski A., Nelson P.F., 2011. Influence of pyrolysis temperature on production and nutrient properties of wastewater sludge biochar. J. Env. Manag. 92, 223-228.

IUSS Working Group WRB, 2007. World Reference Base for Soil Resources, first update 2007. World Soil Resources Reports 103. FAO, Rome.

Kim S., Kramer R.W., Hatcher P.G, 2003. Graphical method for analysis of untrahigh-resolutuon broadband mass spectra of natural organic matter, the vam Krevelen Diagram. Anal. Chem. 75, 5336-5344.

Kishimoto S., Sugiura G., 1985. Charcoal as a soil conditioner. Symposium on Forest Products Research. Int. Achiev. Fut. 5, 1-15.

Knicker H., 2010. "Black nitrogen" - an important fraction in determining the recalcitrance of charcoal. Org. Geochem. 41, 947-950

Knicker H., 2011. Pyrogenic organic matter in soil: Its origin and occurrence, its chemistry and survival in soil environments. Quat. Int. 243, 251-263.

Knicker H., Totsche K.-U., Almendros G., González-Vila F.J., 2005. Condensation degree of burnt peat and plant residues and the reliability of solid-state VACP MAS 13C NMR spectra obtained from pyrogenic humic material. Org. Geochem. 36, 1359-1377.

Lehmann, J., Joseph, S., 2009. Biochar systems. In: C. J. Lehmann C.J., Joseph,S., (Eds), Biochar for Environmental Management: Science and Technology, Earthscan, London.

Lehmann J., Kern D.C., Glaser B., Woods W.I., 2003. Amazonian Dark Earths: Origin, Properties, Management, Kluwer Academic Publishers, The Netherlands.

Macias F., Arbestain M.C., 2010. Soil carbon sequestration in a changing global environment. Mitigation and Adaptation Strategies for Global Change. 15, 511-529.

Madejon E., López, R., Murillo, J.M., Cabrera, F., 2001. Agricultural use of three (sugar-beet) vinasse composts: effect on crops and chemical properties of

a Cambisol soil in the Guadalquivir river valley (SW Spain). Agr. Ecosyst. Env. 84, 55-65.

Major J., Rondon M., Lehmann J., 2007. Fate of biochar applied to a Colombian savanna Oxisol during the first and second years. International Agrichar Initiative (IAI) 2007 Conference, April 27-May 2 2007, Terrigal, Australia. p. 34.

Mudarra Gómez, J.L., 1988. Reconocimiento de los suelos de la comarca del Aljarafe (Sevilla). Consejo Superior de Investigaciones Científicas, Seville.

Mukherjee, A.,Lal, R., Zimmerman, A.R., 2014. Effects of biochar and other amendments on the physical properties and greenhouse gas emissions of an artificially degraded soil. Sci. Tot. Env. 487, 26-36.

Ogawa M., Okimori Y., 2010. Pioneering works in biochar research, Japan. Australian Journal of Soil Research. 48, 489-500.

Özçimen D., Ersoy_meriçboyu A., 2010. Characterization of biochar and bio-oil samples obtained from carbonization of various biomass materials. Renew. En. 35, 1310-1324.

Schimmelpfenning S., Glaser B., 2012. One step forward toward characterization: some important material properties to distinguish biochars. J. Env. Qual. 41, 1001-1013.

Schimmelpfennig S., Müller, C., Grünhage, L., Koch, C., Kammann, C., 2014. Biochar, hydrochar and uncarbonized feedstock application to permanent grassland—Effects on greenhouse gas emissions and plant growth. Agr. Ecosys. Env. (*in press*). DOI:10.1016/j.agee.2014.03.027

Schnitzer M., 1978. 'Humic substances: chemistry and reactions', in: Schnitzer M. and Khan S.U., Soil organic matter. Elsevier scientific publishing company. Amsterdam. pp 1-58.

Sharma R.K., Wooten J.B., Baliga V.L., Lin X., Chan W.G., Hajaligol M.R., 2004. Characterization of chars from pyrolysis of lignin. Fuel. 83,1469-1482.

Sohi S.P., Lopez-Capel E., Krull E., Bol R., 2009. Biochar, climate change and soil: A review to guide future research. CSIRO Land and Water Science Report 05/09.

Srinath E.G., Pillai S.C., 1966. Phosphorus in Sewage, Polluted Waters, Sludges, and Effluents. Quart. Rev. Biol., 41, 384-407.

van Krevelen D.W.,1950. Graphical-statistical method for the study of structure and reaction processes of coal, Fuel. 29, 269-84.

Van Zwieten L., Kimber S., Morris S., Chan K.Y., Downie A., Rust J., Joseph S., Cowie A., 2010. Effects of biochar from slow pyrolysis of papermill waste on agronomic performance and soil fertility. Plant Soil. 327, 235-246.

Veihmeyer F.J., Hendrickson A.H., 1949. Methods of measuring field capacity and wilting percentages of soils. Soil Sci. 68, 75-94.

Weng W.G., Hasemi Y., Fan W.C., 2006. Predicting the pyrolysis of wood considering char oxidation under different ambient oxygen concentrations. Combust. Flame 145, 723-729.

Wu W., Yang M., Feng Q., McGrouther K., Wang H., Lu H., Chen Y., 2012. Chemical characterization of rice straw-derived biochar for soil amendment. Biomass. Bioenerg. 47, 268-276.

Zaho L., Cao X., Masek O., Zimmerman A., 2013. Heterogeneity of biochar properties as a function of feedstock sources and production temperatures. J. Hazard. Mat. 256-257, 1-9.

Figure captions:

Figure 1. Solid state ^{13}C NMR spectra of biochars 2, 3 and 4. Spinning side bands are marked with asterisks (*).

Figure 2. FT-IR spectra of biochars 1, 2, 3 and 4.

Figure 3. FESEM images of biochar samples. A) Surface topography of Biochar 1; B) High magnified image of biochar 1 showing hollow fibers; C) Surface topography of biochar 2 depicting collapsed structures from plant-derived feedstock; D) Detail of vessel remains from biochar 2; E) General FESEM view of Biochar 3 showing heterogeneous compositions; F) Detail of iron-rich mineral particles on the surface of biochar 3; G) Biochar 4 depicting good anatomical preservation; H) Detail of xylem vessels with scalariform perforation plates.

Figure 4. FESEM images and corresponding EDS spectra of biochar samples. A) Detailed image of mineral crystals deposited on the hollow fibers of biochar 1, and EDS spectrum (spectrum 1) evidencing high content of calcium. B) Detailed FESEM image of the collapsed structures from biochar 2 with significant concentrations of C, O, Si, K and Ca (spectrum 2). C) FESEM image of biochar 3 and corresponding EDS spectrum performed on the surface of this sample revealing heterogeneous chemical composition (Al, Si, P, K, Ca and Fe). D) FESEM image and corresponding EDS spectrum of biochar 4 showing high content of C, K and Ca, typical from wood-derived biochar.

Figure 5. Number of germinated and living plants of pots with soil incubated without and with amendment of biochars 1, 2, 3 and 4 at 10, 20 and 40 t

ha^{-1}. The yields are given per pot (150 g of soil) and as a function of incubation time (days). The error bars show the mean standard deviation.

Figure 6. Cumulative above-ground biomass production of pots with soil incubated with and without addition of biochars 1, 2, 3 and 4 at 10, 20 and 40 t ha^{-1}. The yields are given per pot (150 g of soil) and as function of incubation time (days). The error bars show the mean ± standard deviation.

Supplementary information:

Supplementary Figure 1. The van Krevelen plot for elemental data calculated from the biochar samples.

Foot note. Regional plots of elemental composition from some major biomolecular components on the van Krevelen diagram adapted from previous studies (Kim et al., 2003; van Krevelen, 1950). The arrow designates a pathway for a condensation reaction.

Table 1
Click here to download Table: Table 1_Production details of biochar samples.docx

Table 1. Production details of biochar samples

Details	Biochar 1	Biochar 2	Biochar 3	Biochar 4
Producer & location	Swiss Biochar, Laussane, Switzerland	Sonnenerde GmbH, Austria	Pyreg, Germany	Bodegas Torres, Spain
Feedstock	Mixed wood sieving from wood chip	Paper sludge & wheat husks	Sewage sludge (DM 75%)	Vineyard wood (>1 year old)
Duration of pyrolysis	20 min	20 min	20 min	> 60 min
Temperature	20-620 ºC	20-500 ºC	20-600 ºC	unknown
Inert gas	non	non	non	non
Quenching	With water to 30% water content	With water to 30% water content	With water to 30% water content	non

Table 2

Table 2.Tentative chemical shift assignment of various peaks in a ^{13}C NMR-Spectrum according to Knicker et al., (2005).

ppm	Assignment
-10-45	**Alkyl-C**
45-90	**O- and N-alkyl**
45-60	aliphatic C-N. methoxyl
60-90	alkyl-O (carbohydrates. alcohols)
90-160	**Sp^2-hybridized C**
90-140	aryl-H and aryl-C carbons. olefinic-C
140-160	aryl-O and aryl-N carbons
160-210	**Carbonylic-C/carboxylic-C/amide-C**
160-185	carboxyl and amide-C
185-210	aldehyde and ketone carbons

Table 3
Click here to download Table: Table 3_analysis & properties_rev.docx

Table 3. Macro elemental analysis and physicochemical properties of the four biochars and of Cambisol used for the incubation experiment.

		Elemental analysis (C, H, N, O)							Physicochemical properties							
Sample	**Feedstock**	**C**	**H**	**N**	**O**	**H/C_{at}**	**O/C_{at}**	**C/N**	**pH**		**WHC[a] (%)**		**Ash Content (%) (750°C)**		**SSA_{BET}[b] ($m^2\ g^{-1}$)**	
		($g\ kg^{-1}$)	($g\ kg^{-1}$)	($g\ kg^{-1}$)	($g\ kg^{-1}$)					**S.D.**		**S.D.**		**S.D.**		**S.D.**
BC1	Wood	757±31	18±2	3±0.6	116±13	0.3	0.1	252	10.4	±0.0	266	±16	10.6	±0.2	402.7	±5.2
BC2	Paper-Sludge	509±17	20±2	14±2	206±15	0.5	0.3	37	10.4	±0.1	233	±14	25.1	±1.0	116.9	±2.0
BC3	Sewage-Sludge	179±8	15±3	20±2	92±11	1.0	0.4	9	6.7	±0.2	27	± 5	69.5	±0.3	67.3	±1.3
BC4	Grapevine wood	764±24	29±4	6±1	134±12	0.4	0.2	127	10.3	±0.1	178	±17	6.7	±0.4	≤ 5	
Soil		20±5 (7 OC)	3±0.5	10±2				7	8.6	±0.2	46	± 1	95.2	±0.5		

[a]Water Holding Capacity; [b] Specific Surface Area according to Brunauer-Emmett-Teller (BET) equation; S.D.: Standard Deviation.

Figure 1

Click here to download high resolution image

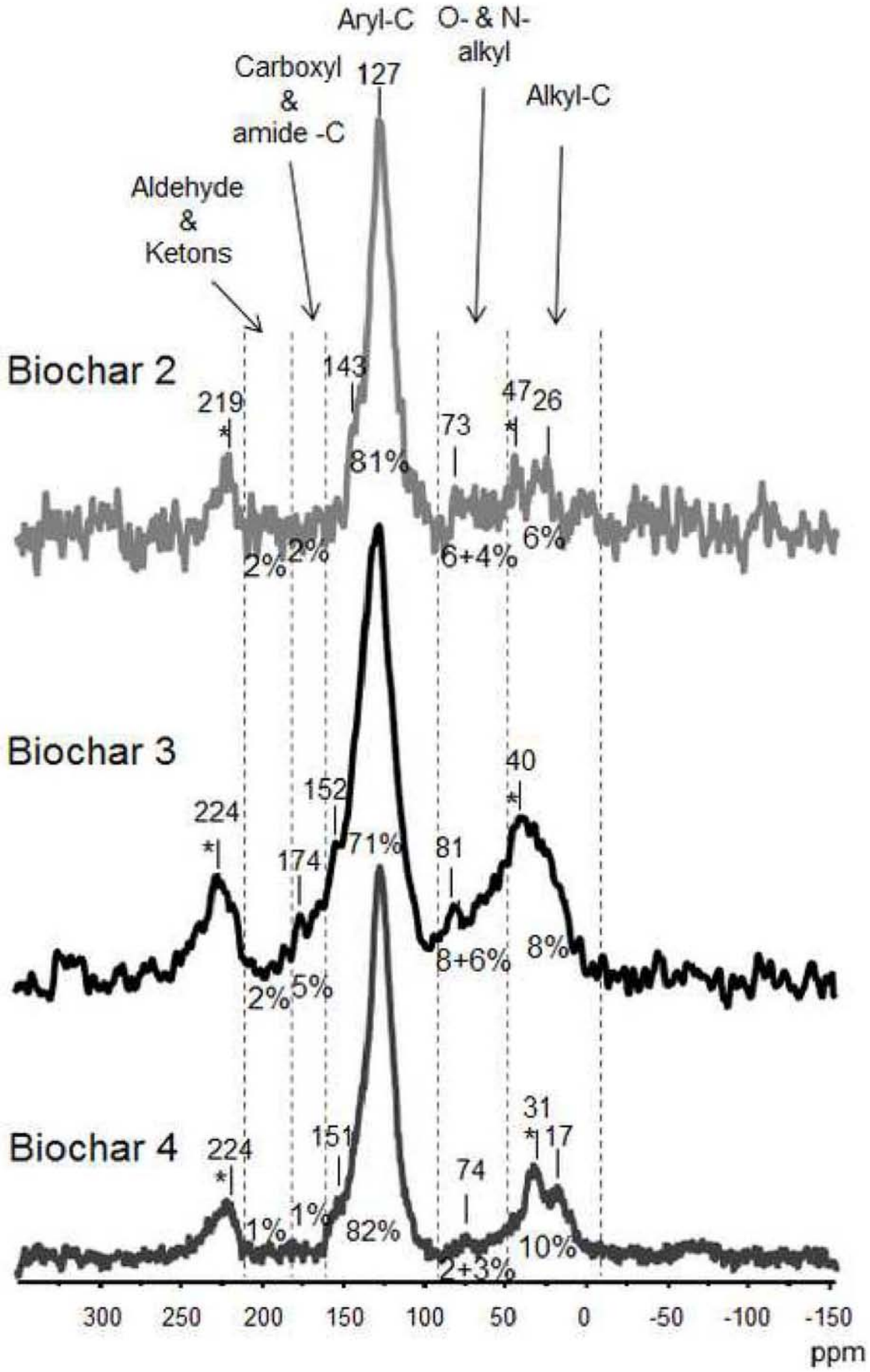

Figure 2

Click here to download high resolution image

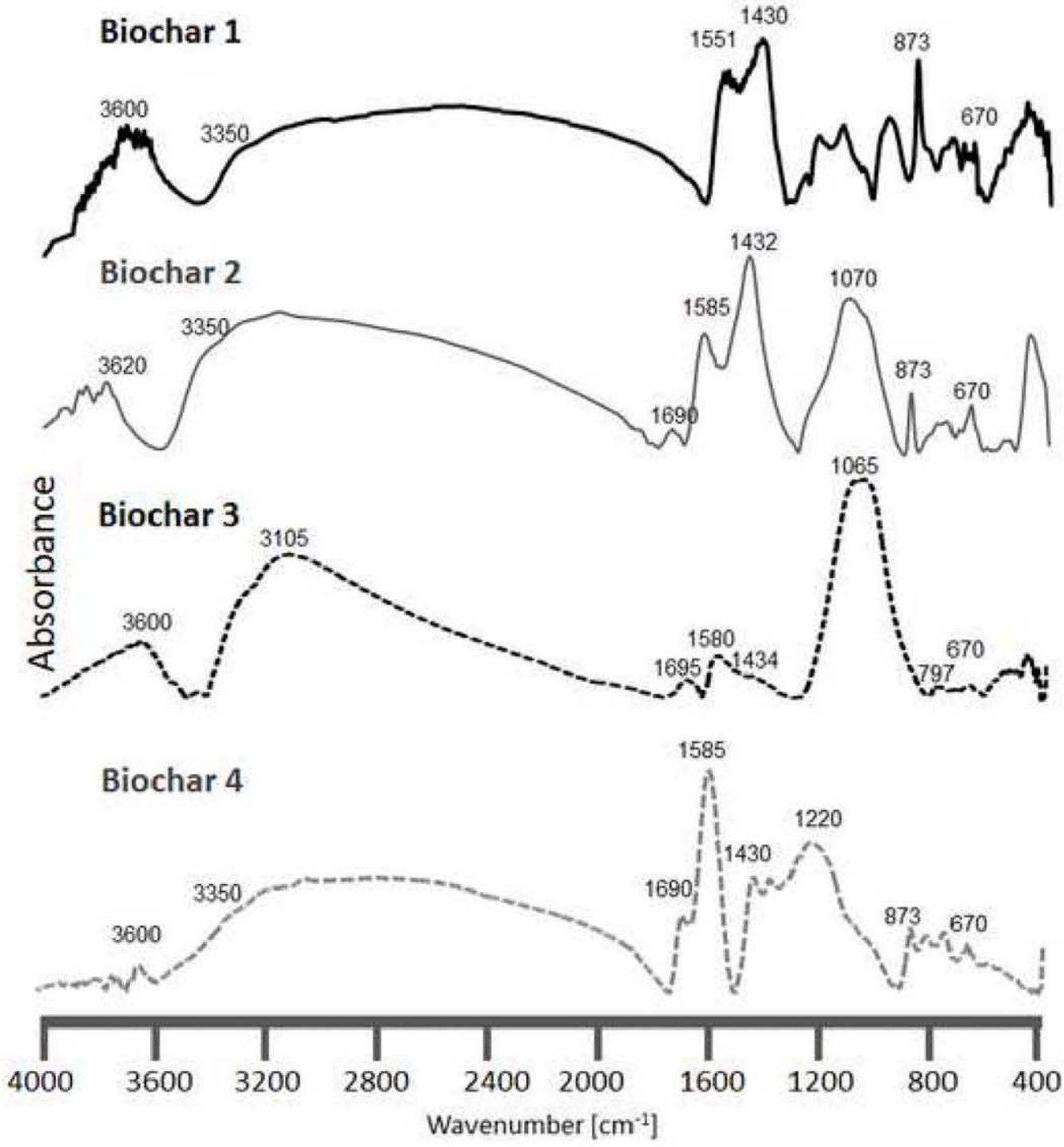

Figure 3

Click here to download high resolution image

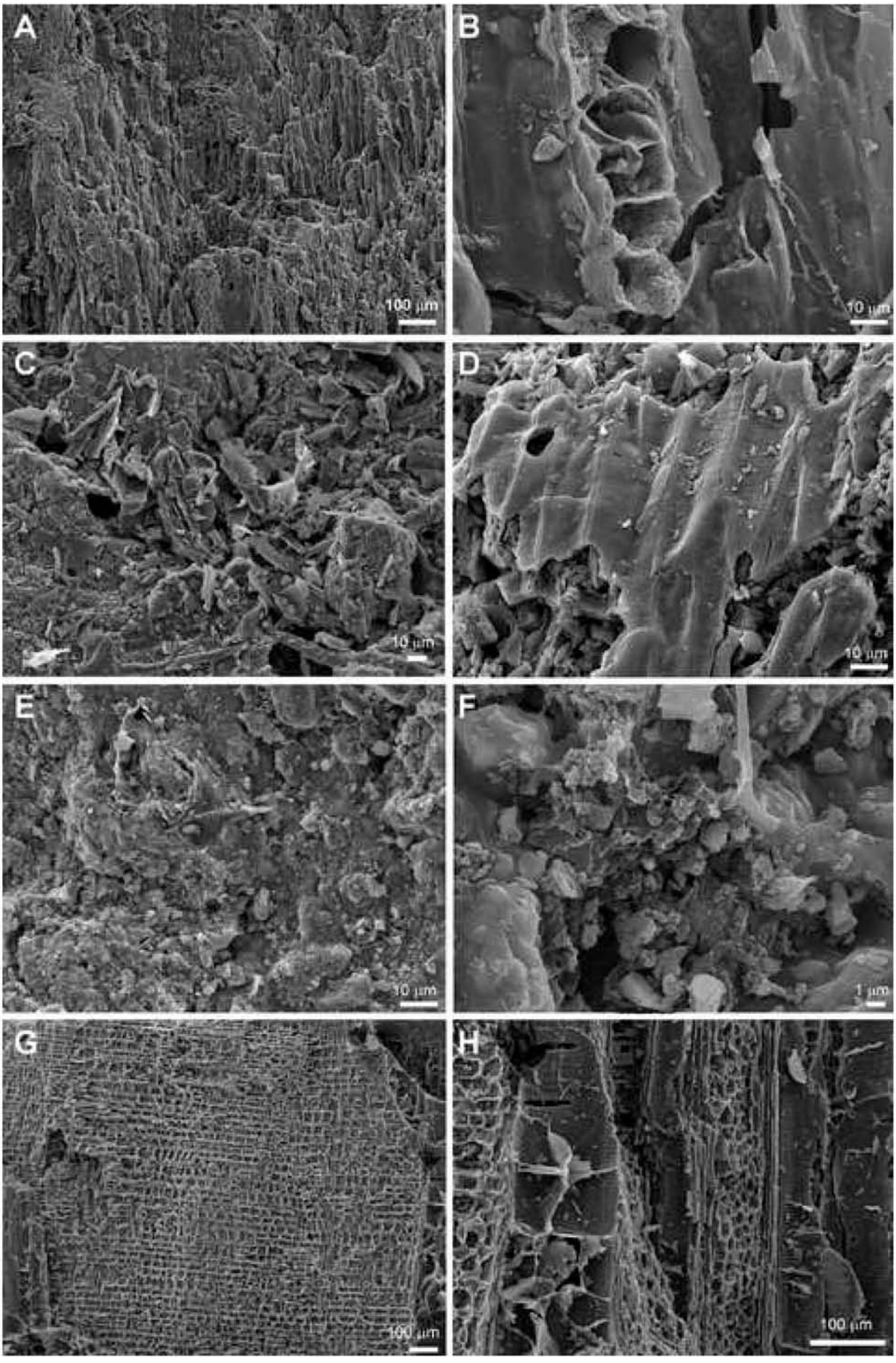

Figure 4

Click here to download high resolution image

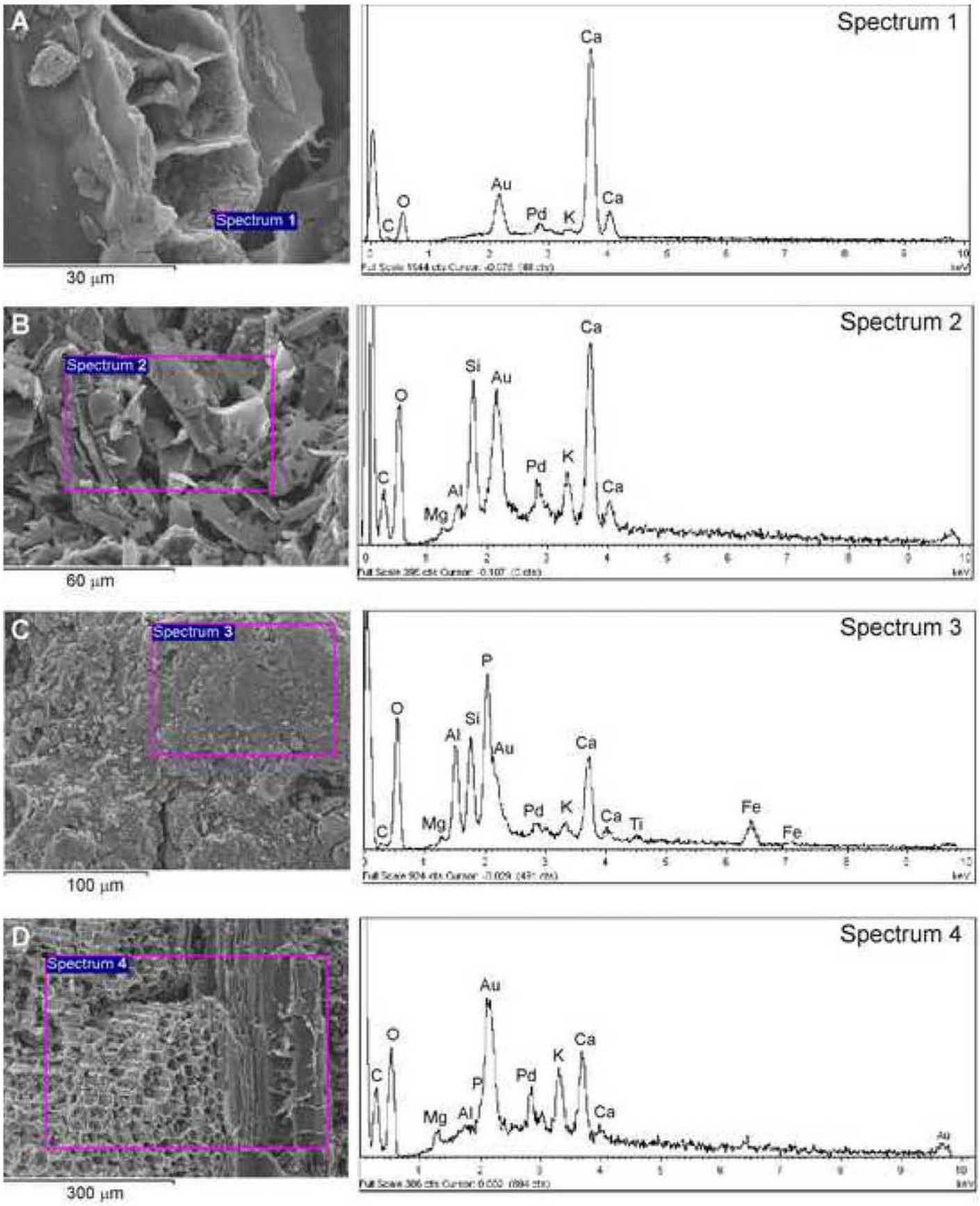

Figure 5
Click here to download high resolution image

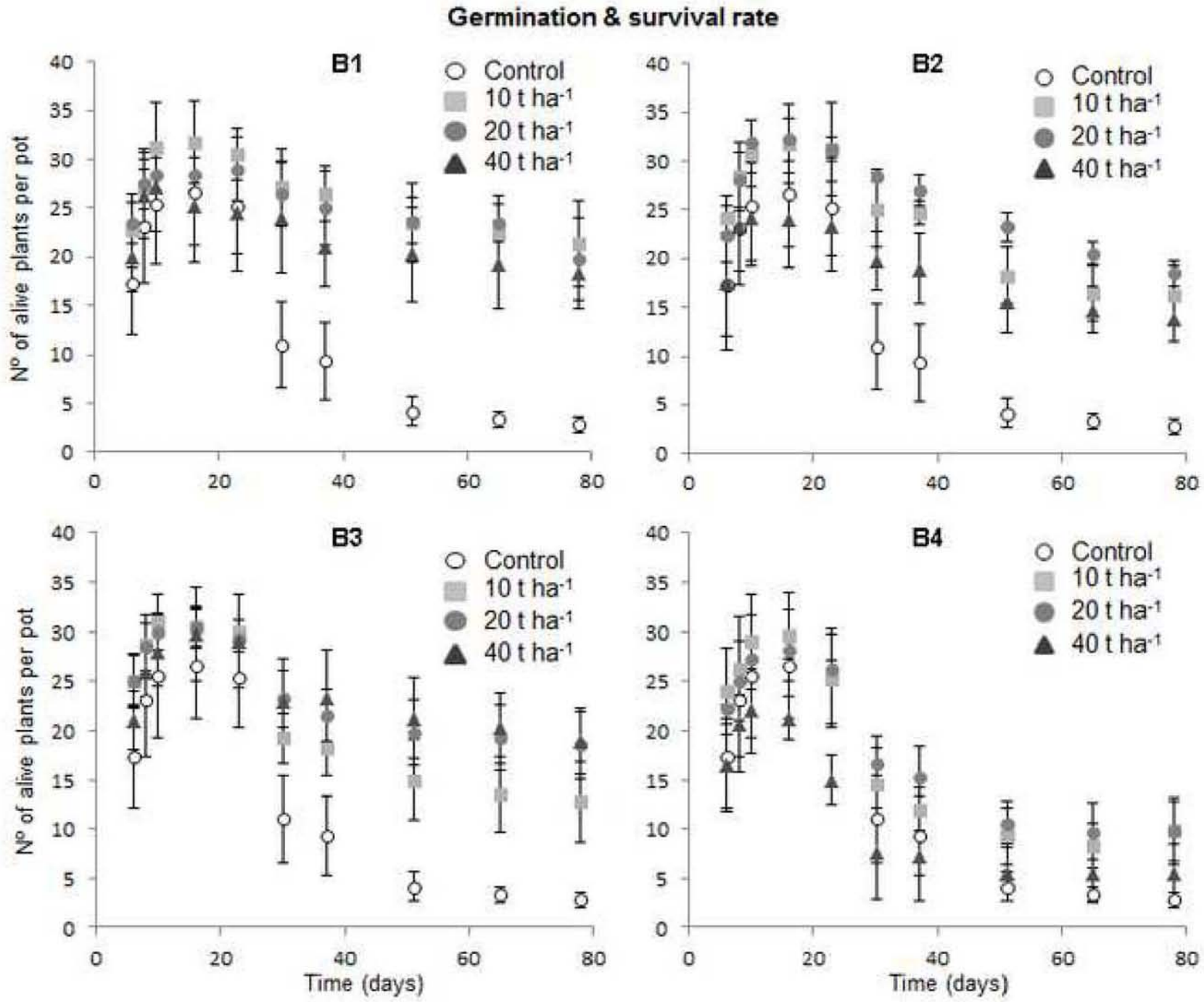

Figure 6
Click here to download high resolution image

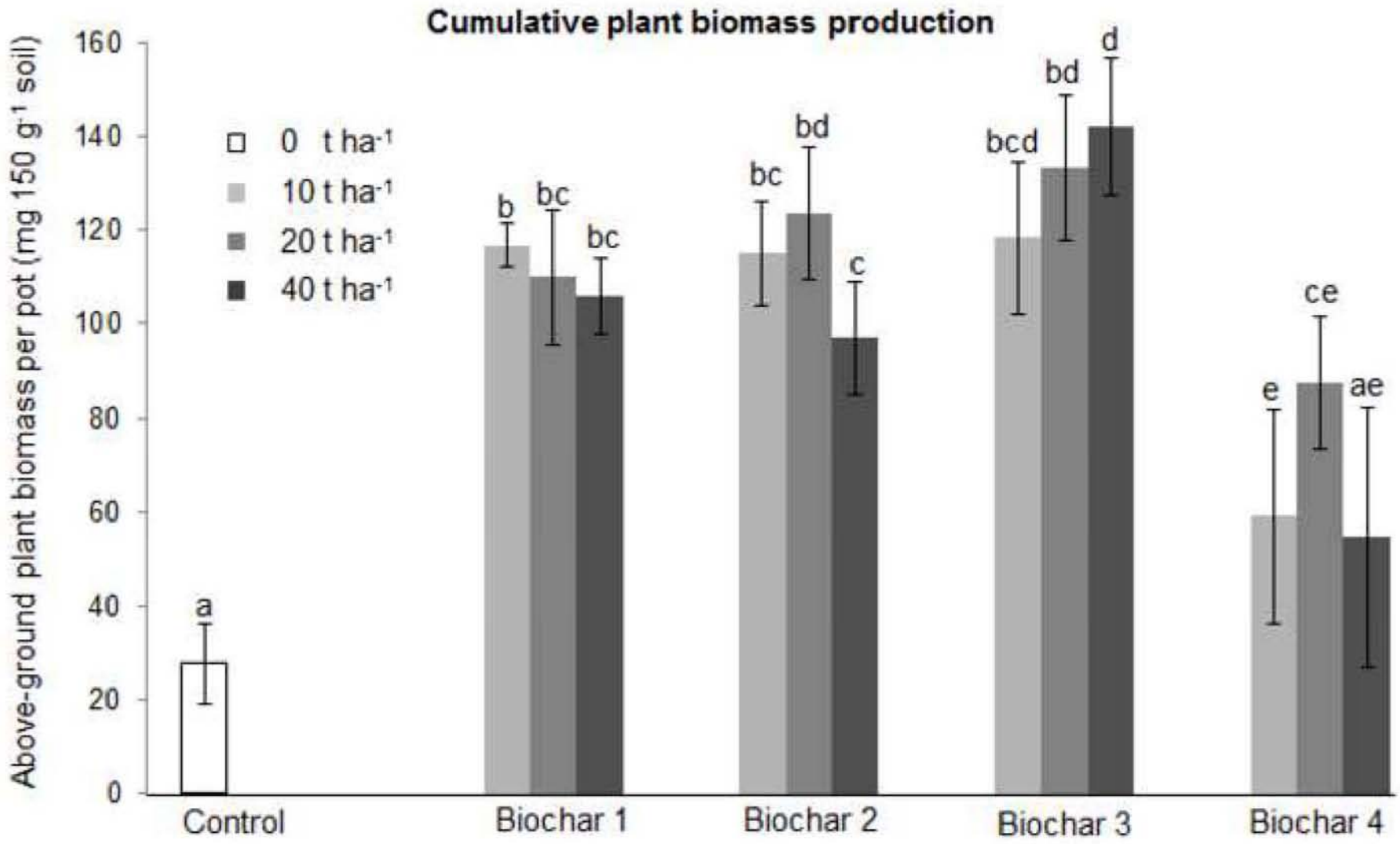

Suplementary figure 1.